A Novel Water-Soluble Tripodal Imidazolyl Ligand as a Model for the Tris(histidine) Motif of Zinc Enzymes: Nickel, Cobalt and Zinc Complexes and a Comparison with Metal Binding in Carbonic Anhydrase

Peter C. Kunz,[a] Guido J. Reiß,[a] Walter Frank,[a] and Wolfgang Kläui*[a]

Dedicated to Professor Bernt Krebs on the occasion of his 65th birthday

Keywords: Bioinorganic chemistry / Cobalt / Enzyme models / N ligands / Nickel / Tripodal ligands / Zinc

Tris[2-isopropylimidazol-4(5)-yl]phosphane (4-TIP^{iPr}), a novel model ligand for the tris(histidine) motif of many zinc enzymes, has been prepared. 4-TIP^{iPr} is hydrolytically stable and soluble in protic solvents. It readily forms chloro- and nitratocobalt, -nickel and -zinc complexes in aqueous methanol. The crystal structures of the solvates [(4-TIP^{iPr})Co(MeOH)(NO$_3$)]NO$_3$·2Et$_2$O (**3**·2Et$_2$O), [(4-TIP^{iPr})Ni(MeOH)(NO$_3$)]NO$_3$·Et$_2$O·MeOH (**4**·Et$_2$O·MeOH), [(4-TIP^{iPr})CoCl]Cl·MeOH·2.5H$_2$O (**5**·MeOH·2.5H$_2$O), and [(4-TIP^{iPr})ZnCl]Cl·MeOH·2.5H$_2$O (**6**·MeOH·2.5H$_2$O) have been determined. The complex **3** shows striking structural similarities to the hydrogencarbonate complex of cobalt-substituted human carbonic anhydrase II (HCA II).

Introduction

In mammalian carbonic anhydrases (CAs) and many other metalloenzymes, the metal-binding site is formed by histidine imidazole rings.[1] In HCA II the three histidine residues His-94, His-96, and His-119 complete a tetrahedral coordination geometry around a Zn−X moiety.

The hydrotris(pyrazolyl)borates (Tp$^{R,R'}$) are the best known of the structural model ligands (Figure 1).[2−4] Their complexes have many of the structural and spectroscopic properties of the active sites of metalloenzymes, though these compounds have been studied mainly in nonprotic solvents, due to the vulnerability of the Tp ligands towards hydrolysis. Attempts to substitute the B−N bonds, to yield more stable ligands, have been made. We have recently re-

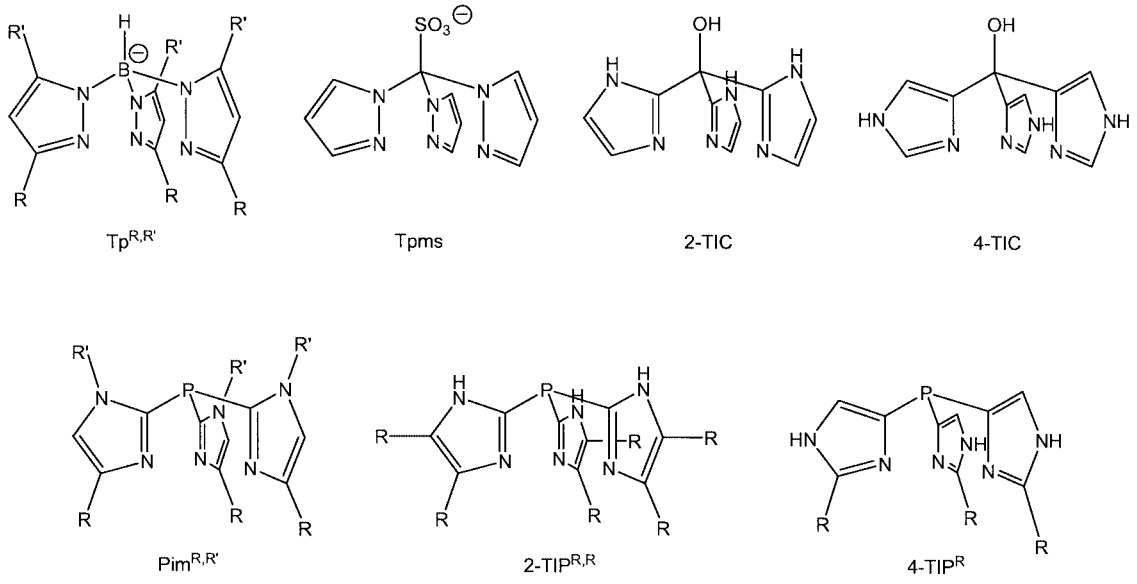

Figure 1. Schematic structures of the novel model ligand 4-TIP^{R} and of related tripodal nitrogen ligands based on pyrazoles and imidazoles

[a] Institut für Anorganische Chemie und Strukturchemie der Heinrich-Heine-Universität Düsseldorf,
Universitätsstr. 1, 40225 Düsseldorf, Germany
Fax: (internat.) + 49-211/8112287
E-mail: klaeui@uni-duesseldorf.de

ported on tris(pyrazolyl)methanesulfonate (Tpms) as a water-soluble Tp-like ligand.[5]

Imidazole ligands should model the actual binding site even better than pyrazole ligands. Attachment of imidazole rings at the 2-position to a molecular framework by the use of 2-lithioimidazoles is relatively simple. In nature, though, the imidazole ring is attached to the histidine side chain through the 4(5)-position. In the early 1980s, Breslow and co-workers synthesized a number of tripodal ligands bearing imidazolyl groups. Tris(imidazol-2-yl)carbinol (2-TIC) and tris(imidazol-4-yl)carbinol (4-TIC), together with M^{2+} complexes (M = Zn, Co) of these ligands, were synthesized as models for the zinc binding site of carbonic anhydrase and alkaline phosphatase.[6,7] Because of the small steric demand of these ligands, however, bis(ligand) formation could not be prevented. Attempts to introduce bulky substituents in the 2-position of 4-TIC resulted in the formation of fulvene-like dehydration products.[7,8]

From Carbinol to Phosphane

Tris(imidazolyl)phosphanes seem to be suitable *N*,*N*,*N*-ligands as models for the active site of the facial His triad in zinc-containing enzymes.[9] Substitution of the central carbinol unit by a phosphorus atom circumvents the dehydration reaction. We have recently reported on tris([2-(1-methyl-4-tolylimidazolyl)]phosphane ($Pim^{Me,pTol}$) and its zinc complexes as structural models of the active site of carbonic anhydrase.[10] The aromatic substituents of this ligand form a hydrophobic cavity around the metal centre and, unlike in the larger substituents, such as the tris(4-*tert*-butyl-1-isopropylimidazol-2-yl)phosphane ($Pim^{iPr,tBu}$),[9] the smaller methyl group in the 1-position provides better solubility in polar solvents.

By this concept, the next step would be not to have any substituent in the 1-position. However, the resulting tris[4(5)-organylimidazol-2-yl]phosphane would undergo prototropic shift reactions. All of the resulting tautomeric forms, after rotation around the phosphorus−carbon bonds, could act as tripodal nitrogen ligands, but with different orientations of the substituents R (Scheme 1).

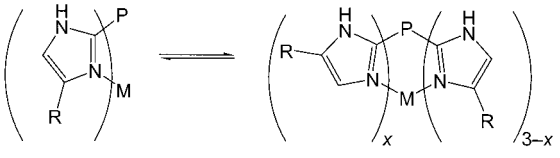

Scheme 1. The different tautomeric forms of tris[4(5)-organylimidazol-2-yl]phosphane; x = 0, 1, 2

This problem can be circumvented by symmetric disubstitution in the 4- and 5-positions of the imidazolyl rings (2-$TIP^{R,R}$),[11] but the introduction of three additional bulky substituents makes these ligands insoluble in protic solvents. To solve this problem we designed an isomeric ligand type, the tris[2-organylimidazol-4(5)yl]phosphanes (4-TIP^{R}s).[12] Here, the prototropic equilibrium and the rotation around the phosphorus−carbon bonds also creates a series of ligands with different binding modes, but only one can now act as a tripodal ligand and here all three substituents R form the desired hydrophobic cavity around the metal ion (Scheme 2).

Below we report on the synthesis of the first member of this class of ligands and of its coordination chemistry toward cobalt, nickel and zinc ions.

Results and Discussion

Synthesis and Spectroscopic Characterisation

2-Isopropylimidazole was protected with an easily removable diethoxymethyl group. In the following step the protected imidazole **1** was lithiated in the 5-position and was then treated with PCl_3 in diethyl ether at −78 °C. Tris[2-isopropylimidazol-4(5)-yl]phosphane (4-TIP^{iPr}, **2**) was isolated as a colourless solid after removal of the protective group (Scheme 3).

The ^{1}H NMR spectrum of **2** in [D_4]methanol shows the expected C_{3v} symmetry of the ligand. The isopropyl groups show a doublet at δ = 1.32 ppm and a septuplet at δ = 3.09 ppm, the signal at δ = 7.00 ppm being assigned to the protons of the imidazolyl rings. In the ^{31}P{^{1}H} NMR spectrum the ^{31}P signal appears as a singlet at δ = −80 ppm. The EI mass spectrum of **2** shows the peak for the molecular ion at the expected *m*/*z* value, together with a characteristic fragmentation pattern.

Cobalt, nickel, and zinc complexes were prepared in high yield by stirring the ligand **2** with the corresponding metal salts in wet methanol at ambient temperature (Scheme 4). The nitrato complexes [(4-TIP^{iPr})M(MeOH)(NO_3)]NO_3 form as violet (**3**) (M = Co) and as grass-green (**4**) (M = Ni) needles, while the chloro complexes [(4-TIP^{iPr})MCl]Cl form as deep blue rhombic (**5**) (M = Co) and colourless crystals (**6**) (M = Zn) by diffusion-controlled crystallisation from diethyl ether in methanolic solutions of the complexes.

The ^{1}H NMR spectrum of **6** has a doublet at δ = 1.39 ppm and a septuplet at δ = 3.62 ppm for the isopropyl groups and a doublet at δ = 7.55 with a $^1J_{PH}$ coupling constant of 2 Hz for the imidazolyl ring protons. The signals of the methyl protons of the isopropyl group show no

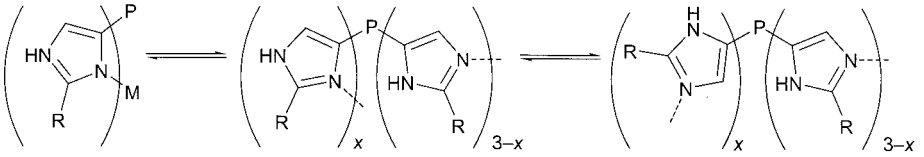

Scheme 2. Of all tris(2-organylimidazol-4(5)yl)phosphanes (4-TIP^{R}s), only one form can act as a tripodal ligand

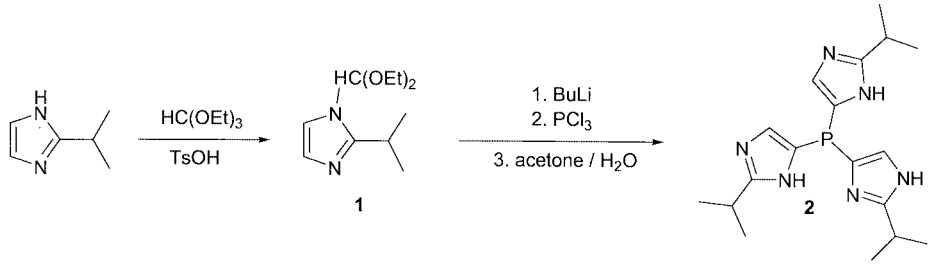

Scheme 3. Synthesis of tris[2-isopropylimidazol-4(5)-yl]phosphane (4-TIP^{iPr}, **2**) from 2-isopropylimidazole

Scheme 4. Synthesis of the nitrato (**3**, **4**) and chloro complexes (**5**, **6**)

significant shift upon coordination, whereas the methine proton of the isopropyl groups and the imidazolyl protons are shifted by about 0.5 ppm to lower field. Upon coordination the ^{31}P NMR signal of the Zn complex **6** is shifted to higher field ($\delta = -106$ ppm), whereas the ^{31}P NMR signals of the cobalt and nickel complexes are shifted to lower field (**3**: $\delta = +27$ ppm; **4**: $\delta = -40$ ppm; **5**: $\delta = -54$ ppm). The NMR spectra of the Co^{II} and Ni complexes show paramagnetic broadening. The FAB mass spectra of all complexes exhibit the peaks for the molecular ions at the expected *m*/*z* values, together with characteristic fragmentation patterns.

The IR spectra of the complexes in nujol and in fluorolube show the characteristic bands of the ligand. Upon preparation of the KBr pellet, the colour of the pellet of the Co^{II} complex turned from violet to deep blue and that of the Ni^{II} complex from green to red. This phenomenon is interpreted in terms of ligand exchange of NO_3^- with Br^- and a simultaneous change in coordination number from 6 to 4 [Equation (1)].

$$[(4\text{-TIP}^{iPr})M(MeOH)(NO_3)]^+ + KBr \rightarrow [(4\text{-TIP}^{iPr})MBr]^+ \quad (1)$$

This interpretation was confirmed by UV/Vis spectra of 1 mM methanolic solutions of **3** saturated with NaX (X = F^-, Cl^-, Br^-, I^-, N_3^-, OAc^-) (Figure 2). The spectrum of $[(4\text{-TIP}^{iPr})Co]^{2+}$ is markedly dependent upon the presence of added anions, indicating association of monovalent anions with the metal ion.

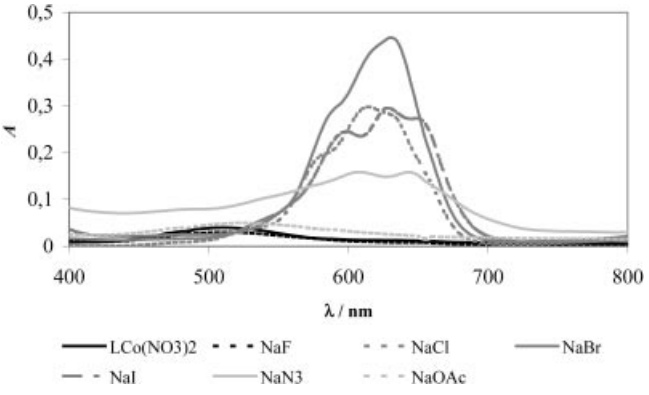

Figure 2. UV/Vis spectra of 1 mM methanolic solutions of **3** saturated with NaX (X = F^-, Cl^-, Br^-, I^-, N_3^-, OAc^-)

Solid-State Structures

The solid state structures of **3**, **4**, **5**, and **6** were determined by crystal structure analysis. The complexes crystallise from wet methanol/diethyl ether. The nitrato complex **3**·2Et_2O crystallises in the triclinic space group $P\bar{1}$, **4**·Et_2O·MeOH in the monoclinic space group $P2_1/c$. The central metal ions in the nitrato complexes are each coordinated facially by three N donor atoms of the 4-TIP^{iPr} li-

gand, in bidentate fashion by the nitrato ligand, and by a methanol molecule to complete the distorted octahedral coordination geometry. Interestingly, the crystal structures each show the expected hydrogen bonds of the imidazolyl N−H protons to solvent molecules. Figure 3 shows an ORTEP plot of **3**·2Et_2O. Selected bond lengths and angles are summarised in Tables 1 and 2.

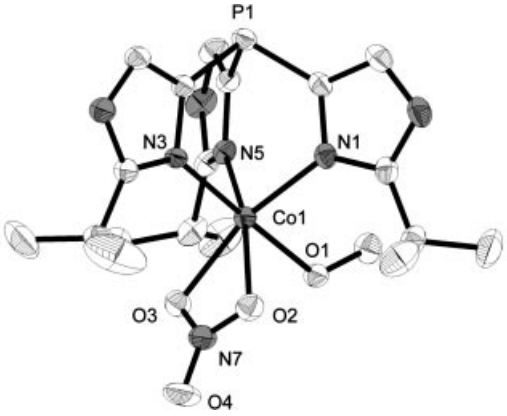

Figure 3. Structure of the cation [(4-TIP^{iPr})Co(HOMe)(NO_3)]$^+$ in **3**·2Et_2O; displacement ellipsoids are shown at the 20% probability level and H atoms are omitted for clarity

Table 1. Selected bond lengths [Å] and angles [°] for [(4-TIP^{iPr})Co(MeOH)(NO_3)]NO_3·2Et_2O (**3**·2Et_2O)

Co1−N1	2.092(3)	Co1−O1	2.167(2)
Co1−N3	2.140(3)	Co1−O2	2.168(3)
Co1−N5	2.096(3)	Co1−O3	2.149(3)
N7−O2	1.271(4)	N7−O3	1.273(4)
N7−O4	1.211(4)		
N1−Co1−N3	88.69(10)	N1−Co1−N5	92.47(12)
N3−Co1−N5	88.50(10)	N1−Co1−O1	90.29(10)
N1−Co1−O2	103.57(12)	N1−Co1−O3	162.76(12)
N3−Co1−O1	178.22(10)	N3−Co1−O2	97.56(10)
N3−Co1−O3	97.29(10)	N5−Co1−O1	90.09(10)
N5−Co1−O2	162.92(12)	N5−Co1−O3	103.79(11)
O1−Co1−O2	84.09(10)	O1−Co1−O3	84.10(10)
O2−Co1−O3	59.70(11)	O2−N7−O3	115.3(3)
O2−N7−O4	122.0(4)	O3−N7−O4	122.8(4)
N7−O2−Co1	92.1(2)	N7−O3−Co1	92.9(2)

The tripodal ligand is bound facially with non-equivalent M−N bond lengths. The M−N bond *trans* to methanol is slightly longer than the M−N bond *trans* to the nitrato ligand [**3**: *d*(Co−N) *trans* to NO_3 ≈ 2.10 Å, *d*(Co−N) *trans* to MeOH = 2.140(3) Å; **4**: *d*(Ni−N) *trans* to NO_3 ≈ 2.04 Å, *d*(Ni−N) *trans* to MeOH ≈ 2.101(3) Å]. Similar behaviour is observed for the M−O bond lengths. The differences in M−O bond lengths and dihedral angles of the NO_3 ligand indicate a bidentate coordination mode ($\Delta d \approx 0.02$ Å; $\Delta\theta$(N−O−M) ≈ 1°).[13]

The chloro complexes **5**·MeOH·2.5H_2O and **6**·MeOH·2.5H_2O crystallise in the monoclinic space group *C2/m*. Figure 4 shows an ORTEP plot of **5**·MeOH·2.5H_2O. Selected bond lengths and angles are summarised in Tables 3 and 4.

Table 2. Selected bond lengths [Å] and angles [°] for [(4-TIP^{iPr})Ni(MeOH)(NO_3)]NO_3·Et_2O·MeOH (**4**·Et_2O·MeOH)

Ni1−N1	2.037(3)	Ni1−O1	2.149(2)
Ni1−N3	2.034(3)	Ni1−O2	2.125(3)
Ni1−N5	2.104(3)	Ni1−O3	2.127(3)
N7−O2	1.264(4)	N7−O3	1.276(4)
N7−O4	1.212(4)		
N1−Ni1−N3	96.23(11)	N1−Ni1−N5	88.41(11)
N3−Ni1−N5	89.48(11)	N1−Ni1−O1	87.69(10)
N1−Ni1−O2	101.92(11)	N1−Ni1−O3	162.03(11)
N3−Ni1−O1	85.74(10)	N3−Ni1−O2	160.42(11)
N3−Ni1−O3	100.68(11)	N5−Ni1−O1	173.47(10)
N5−Ni1−O2	98.23(11)	N5−Ni1−O3	97.73(11)
O1−Ni1−O2	87.70(10)	O1−Ni1−O3	87.54(10)
O2−Ni1−O3	60.58(10)	O2−N7−O3	115.3(3)
O2−N7−O4	123.3(4)	O3−N7−O4	121.5(4)
N7−O2−Ni1	92.3(2)	N7−O3−Ni1	91.8(2)

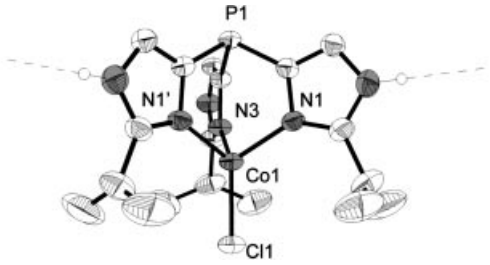

Figure 4. Structure of [(4-TIP^{iPr})CoCl]$^+$ in **5**·MeOH·2.5H_2O; displacement ellipsoids are shown at the 20% level; only the NH hydrogen atoms are shown, others are omitted for clarity; dashed lines indicate the NH−Cl hydrogen bond to the counter-ions in the solid

Table 3. Selected bond lengths [Å] and angles [°] for [(4-TIP^{iPr})CoCl]Cl·MeOH·2.5H_2O (**5**·MeOH·2.5H_2O)

Co1−N1	1.994(4)	Co1−N3	2.013(5)
Co1−Cl1	2.1870(15)		
N1−Co1−N1′	96.0(2)	N1−Co1−Cl1	121.67(9)
N1−Co1−N3	96.21(12)	N3−Co1−Cl1	119.00(13)

Table 4. Selected bond lengths [Å] and angles [°] for [(4-TIP^{iPr})ZnCl]Cl·MeOH·2.5H_2O (**6**·MeOH·2.5H_2O)

Zn1−N1	2.003(4)	Zn1−N3	1.994(6)
Zn1−Cl1	2.160(2)		
N1−Zn1−N1′	92.9(3)	N1−Zn1−Cl1	123.40(13)
N1−Zn1−N3	94.49(16)	N3−Zn1−Cl1	120.47(17)

In the chloro complexes **5**·MeOH·2.5H_2O and **6**·MeOH·2.5H_2O the central metal ion is coordinated tetrahedrally by the 4-TIP^{iPr} ligand and by one of the chloride ions. The angles around the central metal ion deviate significantly from tetrahedral angles; the N−M−Cl angles are larger (119−123°) and the N−M−N angles are smaller (93−96°). In the crystal of **5**·MeOH·2.5H_2O and **6**·MeOH·2.5H_2O, the imidazolyl N−H atoms of the cations

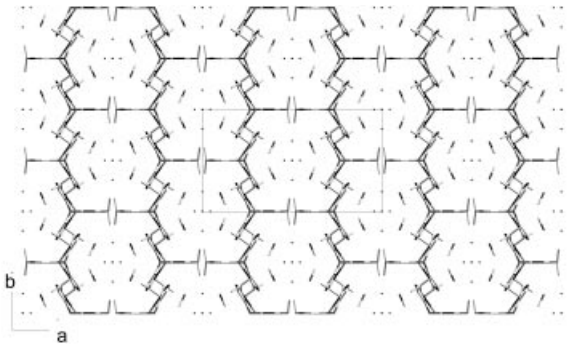

Figure 5. Molecular packing diagram of **5**·MeOH·2.5H_2O; view along the *c* axis; positions of the methanol and water molecules are represented by sticks and single balls; some are partially occupied

form hydrogen bonds to the chloride counter-ion. This results in the formation of hexagonal tubular structures (see Figure 5), filled with solvent molecules showing substantial disorder.

The bond lengths and angles of **6** do not differ significantly from those observed in the X-ray structure of dichloro[tris(4,5-diisopropylimidazol-2-yl)phosphane]zinc(II) bis(*N*,*N*-dimethylformamide).[11b]

The isopropyl groups in all complexes take up a conformation in which the methyl groups point away form the metal centre and the methine protons are oriented towards the metal centre. If this is also the favoured conformation in solution, this would explain the shift of the methine protons in the ^{1}H NMR spectrum of the zinc complex **6**.

Conclusion

We have synthesized the new tris(imidazolyl)phosphane ligand 4-TIP$^{i\mathrm{Pr}}$, which to the best of our knowledge is the first representative of tris[imidazol-4(5)-yl]phosphane ligands. These ligands possess all the minimum features a CA model compound should have: (i) large substituents around the metal centre to suppress bis(ligand) formation and model a hydrophobic cavity, (ii) sufficient solubility in aqueous solvents, and (iii) stability towards hydrolysis.

In 1992, Håkansson and Wehnert reported on the structure of cobalt carbonic anhydrase bearing a hydrogencarbonate ligand.[14] They found that the Co^{II} ion is coordinated by three histidyl ligands of the enzyme, one water molecule and two oxygen atoms of hydrogencarbonate. The structure of **3** shows exactly this motif: Co^{II} is coordinated in a distorted octahedral fashion by the three imidazolyl groups, methanol and two oxygen atoms of nitrate. In **3** we therefore observe a structure in which the coordinated water ligand of the active site of Co^{II}-CA is substituted by methanol and hydrogencarbonate is replaced by the isoelectronic nitrate.

Experimental Section

General: The preparation of the ligand **2** was carried out in Schlenk tubes under dry nitrogen with use of anhydrous solvents purified by standard procedures. The metal complexes were prepared with use of wet solvents. Crystals suitable for X-ray structure analysis were prepared by slow diffusion of diethyl ether into solutions of the complexes in wet methanol. All chemicals were used as purchased. ^{1}H and ^{31}P NMR spectra were recorded with a Bruker DRX 200 spectrometer. The ^{1}H and ^{13}C{^{1}H} NMR spectra were calibrated against the residual proton signals and the carbon signals of the solvents as internal references ([D_1]chloroform: δ_H = 7.30 ppm and δ_C = 77.0 ppm; [D_4]methanol: δ_H = 5.84 ppm and δ_C = 49.1 ppm), while the ^{31}P{^{1}H} NMR spectra were referenced to external 85% H_3PO_4. The EI mass spectra were recorded with a double focussing mass spectrometer, model 311 A Varian MAT, ionisation energy 70 eV. The FAB mass spectra were recorded with a Finnigan mass spectrometer, model MAT 8200, in an NBA matrix. Infrared spectra were recorded with a Bruker IFS 66 FT-IR spectrometer.

Synthesis of *N*-(Diethoxymethyl)-2-isopropylimidazole (1): 2-Isopropylimidazole (22 g, 0.2 mol), triethyl orthoformate (120 g, 0.8 mol), and *p*-toluenesulfonic acid (1 g) were heated at 130 °C for 24 h. Ethanol and excess orthoformate were removed in vacuo, solid Na_2CO_3 (1 g) was added, and the residue was fractionally distilled to yield a colourless oil (26 g, 62%). b.p. 65 °C ($2\cdot10^{-2}$ mbar). ^{1}H NMR ($CDCl_3$, 200 MHz, ppm): δ = 1.13 (t, *J* = 6.8 Hz, 6 H, CH_2CH_3), 1.24 [d, *J* = 6.8 Hz, 6 H, $CH(CH_3)_2$], 3.03 [sept, *J* = 6.8 Hz, 1 H, $CH(CH_3)_2$], 3.3−3.6 (m, 4 H, CH_2CH_3), 5.94 [s, 1 H, $CH(OEt)_2$], 6.83 (d, *J* = 1.3 Hz, 1 H, 4-*H* im), 6.98 (d, *J* = 1.3 Hz, 1 H, 5-*H* im). ^{13}C NMR ($CDCl_3$, 500 MHz, ppm): δ = 15.2 (CH_3CH_2), 22.4 [$(CH_3)_2CH$], 27.0 [$(CH_3)_2CH$], 62.0 (CH_3CH_2), 101.2 [$CH(OEt)_2$], 116.3 (C5 im), 127.2 (C4 im), 153.1 (C2 im). EI MS (70 eV, 30 °C): *m*/*z* (%) = 212 (3) $[M]^+$, 167 (11) $[M - OEt]^+$, 103 (99) $[HC(OEt)_2]^+$.

Synthesis of Tris[2-isopropylimidazol-4(5)-yl]phosphane (4-TIP$^{i\mathrm{Pr}}$) (2): *n*-Butyllithium in hexane (1.6 M, 33 mL, 53 mmol) was added at −78 °C to a solution of **1** (10.6 g, 50.0 mmol) in diethyl ether (300 mL). The solution was stirred at −78 °C for 30 min and additionally at room temperature for 30 min. After the mixture had been cooled to −78 °C, PCl_3 (1.49 mL, 16.7 mmol) in diethyl ether (10 mL) was added. The white suspension was stirred at room temperature overnight, concd. aqueous ammonia (75 mL) was added, and the organic layer was separated, washed with water, and dried with $MgSO_4$. After removal of the solvent, the oily residue was redissolved in acetone/water (10:1, 100 mL) and heated to reflux for 12 h. The resulting white precipitate was collected and recrystallized from methanol/acetone. Yield: 2.1 g (35%). ^{1}H NMR (200 MHz, [D_4]methanol, ppm): δ = 1.32 [d, *J* = 7 Hz, 6 H, $CH(CH_3)_2$], 3.09 [sept, 1 H, *J* = 7 Hz, $CH(CH_3)_2$], 7.00 (s, 1 H, H_{im}). ^{31}P{^{1}H} NMR (200 MHz, [D_4]methanol, ppm): δ = −80. EI MS (70 eV, 250 °C): *m*/*z* (%) = 358 (30) $[M]^+$, 249 (38) $[M - im^iPr]^+$. $C_{18}H_{27}N_6P_3\cdot H_2O$ (374.42): calcd. C 57.4, H 7.7, N 22.3; found C 58.5, H 7.4, N 22.4.

Synthesis of [(4-TIP$^{i\mathrm{Pr}}$)Co(NO_3)(MeOH)](NO_3) (3): A methanolic solution of **2** (180 mg, 50.0 μmol) and $Co(NO_3)_2\cdot6H_2O$ (145 mg, 50.0 μmol) was stirred for 2 h, diethyl ether was added, and the violet precipitate was washed with additional diethyl ether and dried in vacuo. Yield: 0.23 g (85%). ^{31}P{^{1}H} NMR (200 MHz, [D_4]methanol, ppm): δ = 27 ($h_{1/2}$ = 49 Hz). FAB^+ MS (NBA matrix): *m*/*z* (%) = 479 (100) $[(4\text{-}TIP^{i\mathrm{Pr}})Co(NO_3)]^+$, 416 (46) $[(4\text{-}TIP^{i\mathrm{Pr}})Co - H]^+$. $C_{19}H_{30}CoN_8O_7P_3\cdot H_2O$ (591.43): calcd. C 38.6, H 5.6, N 18.9; found C 38.3, H 5.5, N 18.3.

Synthesis of [(4-TIP$^{i\mathrm{Pr}}$)Ni(NO_3)](NO_3) (4): A methanolic solution of **2** (180 mg, 50.0 μmol) and $Ni(NO_3)_2\cdot6H_2O$ (145 mg, 50.0 μmol)

was stirred for 2 h, diethyl ether was added, and the green precipitate was washed with additional diethyl ether and dried in vacuo. Yield: 0.22 g (65%). $^{31}P\{^1H\}$ NMR (200 MHz, [D$_4$]methanol, ppm): δ = −40 (HWB = 138 Hz). FAB$^+$ MS (NBA-matrix): *m*/*z* (%) = 478 (100) [(4-TIP^{iPr})Ni(NO$_3$)]$^+$. $C_{19}H_{30}N_8NiO_7P_3$·3MeOH (669.30): calcd. C 39.5, H 6.5, N 16.7; found C 41.2, H 6.1, N 16.5.

[(4-TIP^{iPr})CoCl]Cl (5): A methanolic solution of **2** (180 mg, 50.0 μmol) and $CoCl_2$ (65 mg, 50.0 μmol) was stirred for 2 h, diethyl ether was added, and the violet precipitate was washed with additional diethyl ether and dried in vacuo. Yield: 0.18 g (65%). $^{31}P\{^1H\}$ NMR (200 MHz, [D$_4$]methanol, ppm): δ = −54 ($h_{1/2}$ = 91 Hz). FAB$^+$ MS (NBA matrix): *m*/*z* (%) = 479 (100) [(4-TIP^{iPr})CoCl]$^+$, 416 (8) [(4-TIP^{iPr})Co − H]$^+$. $C_{18}H_{27}Cl_2CoN_6P_3$·MeOH·H$_2$O (538.32): calcd. C 45.3, H 6.5, N 15.1; found C 45.4, H 6.2, N 14.6.

[(4-TIP^{iPr})ZnCl]Cl (6): A methanolic solution of **2** (180 mg, 50.0 μmol) and $ZnCl_2$ (68 mg, 50.0 μmol) was stirred for 2 h, diethyl ether was added, and the colourless precipitate was washed with additional diethyl ether and dried in vacuo. Yield: 0.10 g (40%). ^1H NMR (200 MHz, [D$_4$]methanol, ppm): δ = 1.39 [d, *J* = 7 Hz, 6 H, CH(C*H*$_3$)$_2$], 3.62 [sept, *J* = 7 Hz, 1 H, C*H*(CH$_3$)$_2$], 7.55 (d, J_{PH} = 2 Hz, 1 H, H$_{im}$). $^{13}C\{^1H\}$ NMR (500 MHz, [D$_4$]methanol, ppm): δ = 21.7 [CH(*C*H$_3$)$_2$], 29.3 [*C*H(CH$_3$)$_2$], 104.3, 125.6 (d, *J* = 56 Hz), 133.3, 159.9 (*C*2$_{im}$). $^{31}P\{^1H\}$ NMR (200 MHz, [D$_4$]methanol, ppm): δ = −106 ($h_{1/2}$ = 3 Hz). FAB$^+$ MS (NBA matrix): *m*/*z* (%) = 457 (100) [(4-TIP^{iPr})ZnCl]$^+$. $C_{18}H_{27}Cl_2ZnN_6P$·MeOH (526.76): calcd. C 43.5, H 5.9, N 16.0; found C 43.1, H 5.7, N 16.4.

X-ray Crystallographic Study: Crystal structure determinations of compounds **3**·2Et$_2$O, **4**·Et$_2$O·MeOH, **5**·MeOH·2.5H$_2$O, and **6**·MeOH·2.5H$_2$O: Crystals suitable for X-ray study were selected by use of a polarisation microscope and investigated with area detector diffractometers by use of graphite-monochromatized Mo-K_α radiation (λ = 0.71073 Å). Unit cell parameters were determined by least-squares refinements on the positions of 6449, 3557, 8000, and 8000 reflections in the range 4° < θ < 25.1°, 4° < θ < 25.5°, 2° < θ < 22.9°, and 2° < θ < 25.8°, respectively. For **3**·2Et$_2$O, $P\bar{1}$ was confirmed to be the correct one of the two triclinic space groups in the course of refinement. Space group type no. 14 was uniquely determined in the case of **4**·Et$_2$O·MeOH. For the isotypical compounds **5**·MeOH·2.5H$_2$O and **6**·MeOH·2.5H$_2$O, systematic extinctions were consistent with space group types *I*2, *Im*, and *I*2/*m*. In accordance with E-statistics, significantly better results were

Table 5. Crystal data for **3**·2*E*t$_2$O, **4**·Et$_2$O·MeOH, **5**·MeOH·2.5H$_2$O, and **6**·MeOH·2.5H$_2$O

	3·2Et$_2$O	**4**·Et$_2$O·MeOH	**5**·MeOH·2.5H$_2$O	**6**·MeOH·2.5H$_2$O
Empirical formula	$C_{27}H_{51}CoN_8O_9P$	$C_{24}H_{45}N_8NiO_9P$	$C_{19}H_{36}Cl_2CoN_6O_{3.5}P$	$C_{19}H_{36}Cl_2N_6O_{3.5}PZn$
M_r	721.66	679.36	565.34	571.78
Crystal system	triclinic	monoclinic	monoclinic	monoclinic
Space group	$P\bar{1}$	$P2_1/c$	*C*2/*m*	*C*2/*m*
Z	2	4	4	4
Temperature [K]	293	293	293	293
Unit cell dimensions				
a [Å]	10.1416(10)	16.738(3)	20.8949(19)	20.962(4)
b [Å]	12.4194(11)	12.3251(15)	11.5197(13)	11.4751(19)
c [Å]	15.5836(16)	17.523(3)	15.1453(14)	15.056(3)
α [°]	91.649(8)	90	90	90
β [°]	100.255(8)	106.020(14)	103.825(11)	103.82(2)
γ [°]	94.649(8)	90	90	90
Volume [Å^3]	1923.2(3)	3474.6(8)	3539.9(6)	3516.7(11)
$D_{calcd.}$	1.246	1.299	1.061	1.080
Absorption coefficient	0.542	0.660	0.706	0.921
F(000)	766	1440	1184	1196
Crystal size [mm]	0.4 × 0.35 × 0.3	0.45 × 0.4 × 0.3	0.35 × 0.35 × 0.35	0.32 × 0.35 × 0.35
Crystal colour	violet	green	blue	colourless
Diffractometer type	Stoe-CCD	Stoe-CCD	Stoe-IPDS	Stoe-IPDS
Crystal−detector distance [mm]	80	80	70	70
Scan mode	ω (21 runs)	ω (21 runs)		
Θ range for data collection [°]	4.08−25.05	4.09−25.50	2.15−24.99	2.15−24.99
Limiting indices	$-12 < h < 12$	$-20 < h < 20$	$-24 < h < 24$	$-23 < h < 24$
	$-14 < k < 14$	$-14 < k < 14$	$-13 < k < 13$	$-13 < k < 13$
	$-18 < l < 18$	$-21 < l < 21$	$-18 < l < 18$	$-17 < l < 17$
Reflections collected	26584	47473	22973	12328
Reflections unique	6765	6420	3263	3201
Reflections observed	5417	5097	2341	1426
Criterion for observation	$I > 2\sigma(I)$	$I > 2\sigma(I)$	$I > 2\sigma(I)$	$I > 2\sigma(I)$
Completeness	0.994	0.995	0.992	0.978
Refined parameters	425	397	183	183
R_1[a], observed	0.0614	0.0633	0.0533	0.0574
wR_2[b], all data	0.1268	0.1158	0.1298	0.1398
Goodness-of-fit, *S*[c]	1.018	1.037	1.097	1.087
Largest diff. peak/hole	0.75/−0.43	0.61/−0.32	0.32/−0.23	0.57/−0.40
CCDC identifier	208101	208102	208099	208100

[a] $R_1 = ||F_o| - |F_c||/|F_o|$. [b] $wR_2 = \{w(F_o^2 - F_c^2)^2/w(F_o^2)^2]^{1/2}\}$, where $w = 1/[\sigma^2(F_o^2) + (aP^2)]$ and $P = (F_o^2 + 2F_c^2)/3$. [c] $S = [w(F_o^2 - F_c^2)^2/(n - p)]^{1/2}$.

observed for disordered models in the centrosymmetric type *I*2/*m*. All data sets were corrected for Lorentz and polarization effects. The structures were solved by direct methods[15] and subsequent ΔF-syntheses. Approximate positions of the hydrogen atoms of all the complex cations were found in different stages of the refinements by full-matrix, least-squares calculations on F^2.[16] The hydrogen atom positions of the uncoordinated solvent molecules needed to be calculated with account being taken of plausible hydrogen bonding. In all cases refinements suffered from the high mobility of the incorporated solvent molecules, and appropriate distance and displacement parameter restraints and constraints had to be applied in order to achieve convergence. Anisotropic displacement parameters were refined for all atoms heavier than hydrogen, with the exception of the carbon and oxygen atoms of the highly mobile solvent molecules of **5**·MeOH·2.5H_2O and **6**·MeOH·2.5H_2O. For the OH group of the methanol molecule of **3**·2Et_2O a weak O−H bond length restraint was applied and the isotropic displacement parameter of the H atom were refined. With idealised bond lengths and angles assumed for the CH_3, CH_2, CH, NH groups of all the compounds, as well as for the methanol and water molecules of **4**·Et_2O·MeOH, **5**·MeOH·2.5H_2O, and **6**·MeOH·2.5H_2O, the riding model was applied for the H atoms. In addition, the H atoms of the CH_3 groups of **3**·2Et_2O and **4**·Et_2O·MeOH were allowed to move collectively around the neighbouring C−C axis. In the case of **4**·Et_2O·MeOH the H atoms of the OH groups of the methanol molecules were also given allowance for rotation around the neighbouring O−C axis. Isotropic displacement parameters of H atoms were kept equal to 120% of the equivalent isotropic displacement parameters of the parent O, N, and C atoms for the NH, CH, and CH_2 groups and equal to 150% for the CH_3 groups, the water molecules and the OH group of the methanol molecule in **4**·Et_2O·2MeOH. Scattering factors, dispersion corrections and absorption coefficients were taken from International Tables for Crystallography (1992, vol. C, Tables 6.114, 4.268, and 4.2.4.2). Details are listed in Table 5. CCDC-208099 to -208102 contain the supplementary crystallographic data for this paper. These data can be obtained free of charge at www.ccdc.cam.ac.uk/conts/retrieving.html [or from the Cambridge Crystallographic Data Centre, 12 Union Road, Cambridge CB2 1EZ, UK; Fax: (internat.) + 44-1223/336-033; E-mail: deposit@ccdc.cam.ac.uk].

Acknowledgments

We thank the Deutsche Forschungsgemeinschaft (DFG) and the Fonds der Chemischen Industrie for financial support.

[1] D. W. Christianson, C. A. Fierke, *Acc. Chem. Res.* **1996**, *29*, 331−339; S. Lindskog, *Pharmacol. Ther.* **1997**, *74*, 1−20.
[2] S. Trofimenko, *Scorpionates − The Coordination Chemistry of Polypyrazolylborate Ligands*, Imperial College Press, London, **1999** and references therein.
[3] G. Parkin, *Chem. Commun.* **2000**, 1971−1985.
[4] H. Vahrenkamp, *Acc. Chem. Res.* **1999**, *32*, 589−596.
[5] [5a] W. Kläui, M. Berghahn, G. Rheinwald, H. Lang, *Angew. Chem.* **2000**, *112*, 2590−2592; *Angew. Chem. Int. Ed.* **2000**, *39*, 2464−2466. [5b] W. Kläui, M. Berghahn, W. Frank, G. J. Reiß, T. Schönherr, G. Rheinwald, H. Lang, *Eur. J. Inorg. Chem.* **2003**, *10*, 2059−2070.
[6] C. C. Tang, D. Davalian, P. Huang, R. Breslow, *J. Am. Chem. Soc.* **1978**, *100*, 3918−3922.
[7] R. Breslow, J. T. Hunt, R. Smiley, T. Tarnowski, *J. Am. Chem. Soc.* **1983**, *105*, 5337−5342.
[8] Similar problems have been observed in the attempted preparation of 4,5-disubstituted tris(imidazol-2-yl)carbinols: R. S. Brown, J. Huguet, *Can. J. Chem.* **1980**, *58*, 889−901.
[9] [9a] C. Kimblin, W. E. Allen, G. Parkin, *Chem. Commun.* **1995**, 1813−1815. [9b] C. Kimblin, V. J. Murphy, G. Parkin, *Chem. Commun.* **1996**, 235−236. [9c] C. Kimblin, B. M. Bridgewater, D. G. Churchill, G. Parkin, *J. Chem. Soc., Dalton Trans.* **2000**, 2191−2194. [9d] C. Kimblin, V. J. Murphy, T. Hascall, B. M. Bridgewater, J. B. Bonanno, G. Parkin, *Inorg. Chem.* **2000**, *39*, 967−974.
[10] W. Kläui, C. Piefer, G. Rheinwald, H. Lang, *Eur. J. Inorg. Chem.* **2000**, *7*, 1549−1555.
[11] [11a] J. Huguet, R. S. Brown, *J. Am. Chem. Soc.* **1980**, *102*, 7572−7574. [11b] R. J. Read, M. N. G. James, *J. Am. Chem. Soc.* **1981**, *103*, 6947−6952. [11c] R. S. Brown, N. J. Curtis, J. Huguet, *J. Am. Chem. Soc.* **1981**, 6953−6959. [11d] R. S. Brown, D. Salmon, N. J. Curtis, S. Kusuma, *J. Am. Chem. Soc.* **1982**, *104*, 3188−3194. [11e] R. S. Brown, M. Zamkani, J. L. Cocho, *J. Am. Chem. Soc.* **1984**, *106*, 5222−5228. [11f] R. G. Ball, R. S. Brown, J. L. Cocho, *Inorg. Chem.* **1984**, *23*, 2315−2318.
[12] We use the acronyms 4-TIP^R and 2-TIP^{R,R} here in analogy to 4-TIC and 2-TIC, an abbreviation introduced by Breslow.[6]
[13] G. J. Kleywegt, W. G. R. Wiesmeijer, G. J. Van Driel, W. L. Driessen, J. Reedijk, J. H. Noordik, *J. Chem. Soc., Dalton Trans.* **1985**, 2177−2184.
[14] K. Håkansson, A. Wehnert, *J. Mol. Biol.* **1992**, *228*, 1212−1218.
[15] G. M. Sheldrick, *SHELXS-97, Program for the Solution of Crystal Structures*, University of Göttingen, Germany, **1990**.
[16] G. M. Sheldrick, *SHELXL-97, Program for the Refinement of Crystal Structures*, University of Göttingen, Germany, **1997**.

Received April 22, 2003

